Establishment and characteristics of GWH04, a new primary human glioblastoma cell line

FANGLING CHENG[1,2], XUEYAN WAN[3], BAOFENG WANG[3], YOUWEI LI[3], PENG PENG[3], SANPENG XU[4], CHAO HAN[5], FENG MAO[3] and DONGSHENG GUO[3]

[1]Hubei Key Laboratory of Hepato-Pancreato-Biliary Diseases; [2]Hepatic Surgery Centre, Tongji Hospital, Tongji Medical College; [3]Department of Neurosurgery, Tongji Hospital, Tongji Medical College; [4]Institute of Pathology, Tongji Hospital, Tongji Medical College, Huazhong University of Science and Technology, Wuhan, Hubei 430030; [5]Department of Neurosurgery, The First Hospital of Laohekou, Xiangyang, Hubei 441800, P.R. China

Received June 6, 2022; Accepted September 13, 2022

DOI: 10.3892/ijo.2022.5429

Abstract. Glioblastoma multiforme (GBM) is a common and fatal disease of the central nervous system. GBM cell lines are fundamental tools used in GBM research. The establishment of novel continuous GBM cell lines with clear genetic backgrounds could facilitate the exploration of molecular mechanisms and the screening and evaluation of antitumor drugs in GBM studies. In the present study, a novel primary glioblastoma cell line was established, named GWH04, from a patient with GBM, and its STR genotype and various tumor parameters were examined. The STR information of GWH04 was identical to that of the original primary tumor tissue. Compared with existing cell lines, GWH04 had a similar *in vitro* proliferation rate as the U87 cell line, but a faster rate than the GL15 cell line, and substantial soft agar clone-formation capacity and subcutaneous and intracranial tumorigenic capacity. For drug sensitivity test, half maximal inhibitory concentration assays for multiple drugs were performed in these three cell lines, and GWH04 cells were found to be resistant to temozolomide. Aneuploid karyotype with a median of 84 chromosomes was possessed by GWH04, as well as chromosomal structural abnormalities, such as broken chromosomes, double centromere chromosomes, homogeneous staining regions, and double microbodies. Gene sequencing further revealed the mutational status of genes *TP53*, *PTEN*, *PDGFRA*, *ERBB2*, *BRCA1*, *NF1*, and *MLH1* and the promoter region of telomerase reverse transcriptase (C228T) in this cell line. Altogether, these results indicated that GWH04 will be a useful tool for human GBM studies both *in vitro* and *in vivo*.

Correspondence to: Dr Feng Mao, Department of Neurosurgery, Tongji Hospital, Tongji Medical College, Huazhong University of Science and Technology, 1095 Jiefang Avenue, Wuhan, Hubei 430030, P.R. China
E-mail: fengbeyond8@126.com

Key words: glioblastoma, GWH04, primary cell culture, karyotype, tumor xenograft

Introduction

Malignant gliomas are the leading cause of central nervous system tumor-related deaths and affect more than 50% of glioma patients, and patients who are affected by glioblastoma multiforme (GBM) have a poor prognosis, with a mean life expectancy of less than 2 years (1,2). As the overall survival of GBM patients has not improved markedly in the last 20 years, the current gold standard for GBM treatment is only palliative, including surgery, adjuvant radiotherapy, and temozolomide (TMZ) chemotherapy. One of the major hurdles in the development of novel treatment regimens for GBM is the challenge of translating scientific knowledge from bench to bedside, mainly owing to the fact that most research models only poorly replicate the tumor behavior and, consequently, numerous drugs that perform well in glioma models ultimately fail in clinical trials.

To date, malignant glioma cultures, particularly publicly available cell lines, such as those obtained from the American Type Culture Collection (ATCC), represent a useful experimental tool for studies on glioma formation and progression, discovery of new antitumor strategies, and for the identification of molecular markers in response to conventional chemotherapies and targeted agents showing clinical utility. In a search for articles associated with original glioma cell cultures, it was found that cell lines bearing the prefix 'U', such as U251, U87, and U138, were established at Uppsala University, Sweden (3,4), and cell lines bearing the prefix 'LN', such as LN-18, LN-229, and LN-464, were established at the Neurosurgical Service of the University Hospital (CHUV) in Lausanne, Switzerland (5,6). In 1999, Ishii *et al* (7) demonstrated the diagnoses of the original tumors, clinical features of the patients, the mutation status of the associated genes (*TP53*, *PTEN*, *CDKN2A*), and the subcutaneous tumorigenicity of 34 randomly chosen human glioma cell lines, and this was a well comprehensive study of glioma cell lines. Not all of these cell lines are equally used in the present study, and the 19 cell lines of the 34 formed subcutaneous tumor masses in nude mice were used relatively more widespread (7). The tumorigenicity of these GBM cell lines is firmly associated with their popularity in cancer research studies for its advantages *in vivo*

in nude mice, thus, tumorigenic cell lines as U87 and U251 are more widely used than nontumorigenic cell lines such as HS683 and A172 (7,8).

Although the aforementioned cell lines have been established and widely used for more than 40 years, they have several drawbacks that need to be considered. For example, *in vitro* subculture imposes a selection pressure on cell lines, which could result in genetic drift over time. In addition, long-term cultures represent a risk of cross-contamination with other cell lines. The most commonly used cell line, U87, from the ATCC, which has been passaged worldwide for more than 50 years, was found to be different from the original U87 line established in the Uppsala laboratory in 1966 or any other laboratory-established glioma cell line (7,8). Furthermore, U373 and U251 were first established as two different cell lines, but recent short-tandem repeat (STR) identification confirmed that they have the same origin (https://web.expasy.org/cellosaurus/CVCL_0021; https://web.expasy.org/cellosaurus/CVCL_2219). Thus, numerous journals require cell line STR authentication and primary cell culture to ensure the reliability of the studies. Therefore, new cell lines are urgently required to replace those old, long-term-use cell lines.

During the past few years, several adherent primary cultures from freshly resected tissues of patients with different grades of glioma have been routinely conducted; one permanent and tumorigenic cell line without any additional genetic modification, named GWH04, was established from a 72-year-old female patient with GBM. This cell line is suitable for the common culture medium and has been sub-cultured more than 70 times, and cryopreserved at different early-passage stages. In the present study, the establishment of this primary GBM cell line was described and its biological characteristics including proliferation rate, karyotype analysis, half maximal inhibitory concentration (IC_{50}) of different chemotherapy drugs, and glioma-associated gene test, as well as the pathological and histological characteristics of the original tumor from the patient, and the intracranial xenografts in nude mice of this cell line, were presented. This GWH04 cell line (first named Fu) was deposited at the Bio-research Innovation Center of Suzhou (BRICS; http://www.brics.ac.cn/cell/template/cell/cell_detail.html?id=3825), and also preserved in the China Center for Type Culture Collection, Wuhan, China (CCTCC, NO.C202163). Altogether, it will contribute to the diversity of GBM cell lines and will be a useful tool for studies of human GBM both *in vitro* and *in vivo* for all researchers.

Materials and methods

Clinical history and characteristics. In the present study, 10 cases of primary cell cultures from different GBM tumor tissues were comprehensively investigated. Among which, GWH04 cells could well circumvent replicative senescence and acquire the ability to sustain unlimited proliferation in this culture medium. The detailed information of the patient from whom GWH04 cells were derived is presented below.

The 72-year-old woman was admitted to the Neurosurgery Department of Tongji Hospital in November 2016 with a 10-day history of headache and left limb weakness, and 4 days of rapid aggravation since the initial onset. Computerized tomography (CT) and magnetic resonance imaging (MRI) of the brain revealed a lesion occupying the right temporal lobe with large areas of surrounding edema (Fig. 1A-D). Gadolinium-enhanced MRI of the head showed a solid, enhancing lesion on the T1-weighted sequence, with the appearance of an irregular ring (Fig. 1E). The tumor was grossly microscopically resected during surgery, and a histological diagnosis of GBM was made according to the 2007 World Health Organization classification of tumors of the central nervous system. However, the tumor recurred rapidly, and the patient died within 3 months after surgery. Detailed information was given to the relatives of the patient and informed consent was provided prior to surgery. All samples were obtained from the Department of Neurosurgery, Tongji Hospital, Huazhong University of Science and Technology (Wuhan, China) after written informed consent was obtained and according to the protocol approved (approval no. TJ-IBR20210119) by the Research Ethics Committee of Tongji Hospital, Tongji Medical College, Huazhong University of Science and Technology. All procedures involving human samples were in accordance with the 1964 Helsinki Declaration and its later amendments or comparable ethical standards.

Tumor tissue was acquired during the surgery for paraffin tissue embedding, liquid nitrogen cryopreservation, and primary cell culture.

Immunohistochemistry and pathological examination of glioma tissues. Immediately after resection, the tumor samples were fixed in 4% paraformaldehyde, dehydrated with an ethanol gradient, permeabilized with xylene, and embedded in paraffin (25-28˚C). Paraffin-embedded tissue sections (4-μm thick) were generated and stained with hematoxylin and eosin (H&E) at 25-28˚C (Fig. 1F). Continuous tissue sections were generated and immunohistochemically (IHC) stained for glial fibrillary acidic protein (GFAP; cat. no. ZM-0118), NeuN (cat. no. ZM-0352), Olig2 (cat. no. ZA-0561), O6-methylguanine-DNA methyltransferase (MGMT; cat. no. ZM-0461), Nestin (cat. no. ZA-0628), EMA (cat. no. ZM-0071), Syn (cat. no. ZA-0263), c-Myc (cat. no. ZA-0658), EGFR (cat. no. ZM-0093), p53 (cat. no. ZM-0408) and Ki67 (cat. no. ZM-0167; all from OriGene Technologies, Inc.). Antigen retrieval was performed in a microwave with citrate buffer (pH 6.0), and the inactivation of endogenous peroxidase was performed in 3% H_2O_2. Bovine serum album (3%; cat. no. 01010010610; GENVIEW) was added to evenly cover the tissue and block non-specific antigens for 30 min at 25-28˚C. Then, the slides were incubated with primary working solution antibodies at 25-28˚C for 2 h. Then, the sections were incubated with biotin-labeled secondary antibody (working solution; cat. no. DS-0004; OriGene Technologies, Inc.) at 25-28˚C for 50 min and the final signals were developed using 3,3'-diaminobenzidine substrate (R&D Systems, Inc.). The sections were analyzed by optical microscopy after counterstaining with hematoxylin. All procedures and subsequent histological diagnoses were performed in the Pathology Department of Tongji Hospital.

Primary cell culture and authentication. The tumor specimen (<1 cm^3) was obtained shortly after surgery and rinsed twice with phosphate-buffered saline (PBS) to wash out residual red

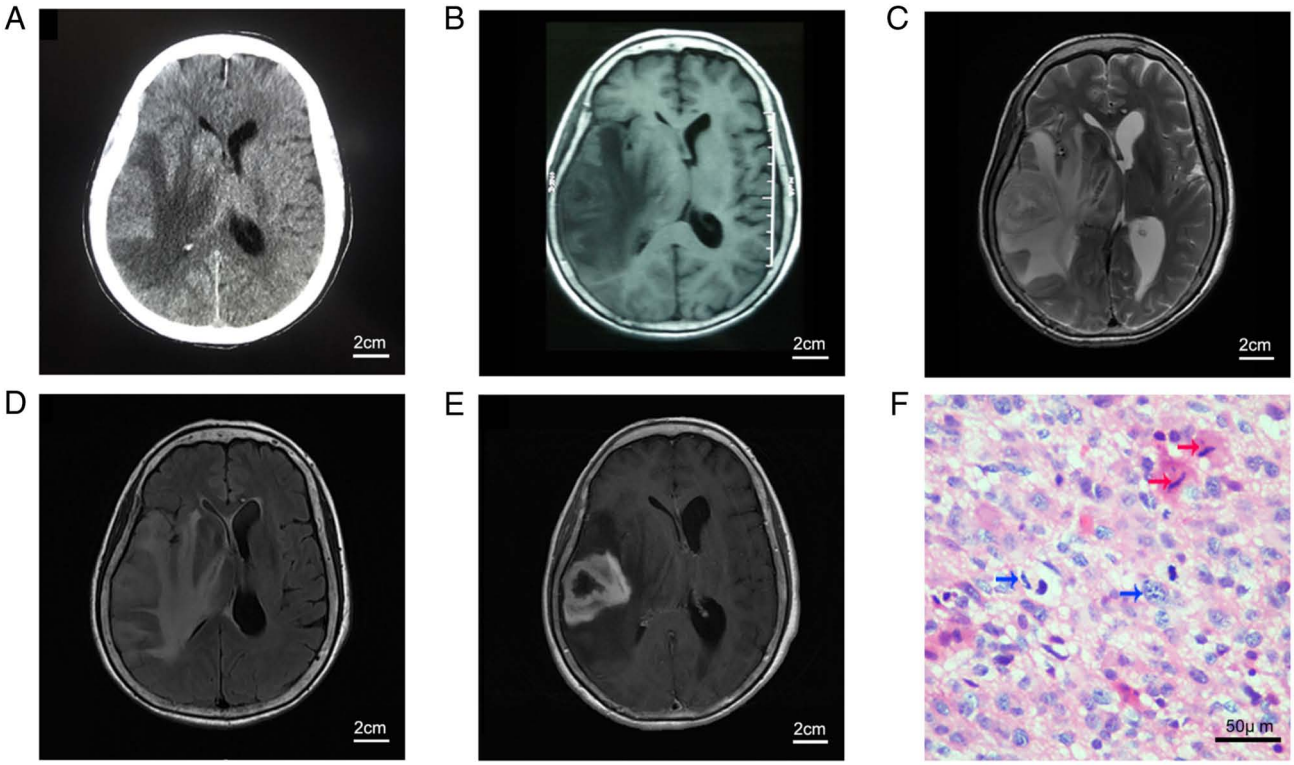

Figure 1. Preoperative imaging and pathologic features of the tumor. (A) Axial computerized tomography scan revealed a space occupying lesion in the right temporal lobe. (B-E) Axial magnetic resonance imaging scan of T1-weighted, T2-weighted, T2-FLAIR and gadolinium-enhanced T1-weighted images, all demonstrated the occupied lesion in the right temporal lobe. (F) H&E stain of the resected tumors, showed numerous nuclear atypia (blue arrow) and mitoses (red arrow).

blood cells. The specimen was prepared as a single cell suspension by mechanical dissociation (1-2 mm) with sterile scissors, treated with 0.125% trypsin (5), and agitated with a horizontal shaker (180 rpm) until the tissue granules became smaller. All suspensions were passed through a sterile filter with a 200-μm pore diameter and centrifuged (300 x g, 5 min, 4˚C). The cell pellets were resuspended in complete medium [10% fetal bovine serum (FBS) + Dulbecco's modified Eagle's medium (DMEM)] and seeded on a 25 cm^2 culture flask as an adherent culture in a humidified incubator with 5% CO_2 at 37˚C.

During the first five passages, only half of the medium was changed each time. When a monolayer of primary tumor cells was formed and reached 90% confluence, they were passaged after 0.25% trypsin digestion, and cultured at 1:3-1:5 dilution in a new flask. After subsequent passages, as with the U251 and U87 cell lines, all stably passaged cells were viably frozen in medium plus 10% dimethyl sulfoxide and stored at -80˚C (5).

For authentication, DNA from cultured cells and primary tumor tissue was isolated using an AxyPrep Multisource Genomic DNA Miniprep kit (Axygen; Corning, Inc.), and 20 STR loci were examined and compared with the corresponding STR profile of the tumor tissue. After bacterial and mycoplasma contamination tests were confirmed negative, the GWH04 cell line (first named as Fu) was deposited at BRICS, and also preserved in the CCTCC.

Immunofluorescence assay of GWH04 cells. Single cell suspensions of GWH04 were seeded into 24-well plates with round glass coverslips. After 24 h, the cells were fixed with 4% paraformaldehyde at room temperature (25-28˚C) for 15 min, permeabilized with 0.25% Triton X-100 for 5 min, and blocked with goat serum (5%, cat. no. WGAR1009-5; Wuhan Servicebio Technology Co., Ltd.) for 1 h. Primary antibodies against GFAP (1:1,000; cat. no. 3670; Cell Signaling Technologies, Inc.) and Nestin (1:5,000; cat. no. 2280493; MilliporeSigma) were added and incubated overnight at 4˚C. Cells were rinsed with PBS, and fluorescence-labeled secondary antibodies (1:100; cat. nos. GB21303 and GB25303; Wuhan Servicebio Technology Co., Ltd.) were added and incubated at room temperature for 1 h. The cells were then stained with DAPI (at 25-28˚C) for 5 min, rinsed with PBS, sealed with a mounting medium, and analyzed using a fluorescence microscope (Olympus Corporation). To compare GFAP levels, cells cultured from pilocytic astrocytoma tissue (grade I), grade II and grade III gliomas were also stained for GFAP under similar staining conditions as those used for GWH04 cells.

Cell lines of U87 and GL15. U87 cell line was purchased from the ATCC with unknown origin (HTB-14), GL15 cell line was donated by Dr Håkan Hedman, Umeå University Hospital, Sweden. Both of these two cell lines were cultured in DMEM/high glucose supplemented with 10% FBS (cat. no. 04-001; BioLegend, Inc.), 100 U/ml penicillin, and 0.1 mg/ml streptomycin in a humidified incubator with 5% CO_2 at 37˚C. The STR identification of the U87 used in the present study was conducted in BRICS institution, and was in consistent with the information presented in the website (https://web.expasy.org/cellosaurus/CVCL_0022).

Cell proliferation and soft agar colony formation assay. Cells (U87, GL15 and the 10, 20, 50th passages of GWH04) were seeded onto 96-well plates at $2x10^3$ cells per well in 100 μl suspensions in triplicate per day and maintained in complete culture medium for 5 days. The cell proliferation rate was measured using the Cell Counting Kit-8 assay (CCK-8; cat. no. KJ800; Dojindo Laboratories, Kumamoto, Japan) according to the manufacturer's instructions. At the time points of attachment (day 0), 24, 48, 72, 96, and 120 h, 10 μl CCK-8 assay reagent was added to each well with 90 μl culture medium and incubated for 1 h at 37˚C. The absorbance was measured with a microplate reader using a wavelength of 450 nm.

For soft agar assays, 0.5% Basal Medium Eagle (BME) agar, containing 10% FBS, 2 mM L-glutamine, and 25 μg/ml gentamicin, was added to six-well plates (3 ml/well), with triplicates per cell line. The plates were then placed in an incubator for 1 h to coagulate the semi-solid medium. Subsequently, GWH04 cells were resuspended at a concentration of $9x10^3$/ml in 0.33% BME agar containing 10% FBS, and seeded at 1 ml/well. The cultures were maintained at 37˚C in a 5% CO_2 incubator for 14 days, and the cell colonies (>25 μm) of bright field were observed via microscopy. The number of colonies and their relative diameters were manually recorded and analyzed.

IC_{50} tests. In the present study, TMZ (cat. no. HY-17364), lomustine (CCNU; cat. no. HY-13669), irinotecan (SN-38; cat. no. HY-13704), etoposide (VP-16; cat. no. HY-13629), 5-fluorouracil (5-Fu; cat. no. HY-90006), oxaliplatin (cat. no. HY-17371), gefitinib (cat. no. HY-50895), BIBR1532 (cat. no. HY-17353), olaparib (cat. no. HY-10162) were selected for drug sensitivity tests (all purchased from MedChemExpress). A total of 8-11 concentration gradients were set of each drug according to the results of pre-experiments (TMZ: 1, 10, 20, 40, 80, 160, 320, 640, 1,280 and 2,560 μM; CCNU: 1, 2, 4, 8, 16, 32, 64, 128 and 256 μM; SN-38: 0.001, 0.01, 0.1, 1, 2, 5, 10, 20, 40, 80 and 160 nM; VP-16: 0.1, 1, 2, 5, 10, 20, 40 and 80 μM; 5-Fu: 0.1, 1, 2, 5, 10, 20, 40, 80, 160 and 320 μM; oxaliplatin: 0.01, 0.1, 1, 5, 10, 20, 40, 80, 160 and 320 μM; gefitinib: 0.1, 0.5, 1, 2, 5, 10, 20, 40, 80 and 100 μM; BIBR1532: 0.1, 1, 5, 10, 20, 40, 80, 160 and 320 μM; olaparib: 0.1, 1, 2, 5, 10, 20, 40, 80, 160 and 320 μM). GWH04, U87 and GL15 cells were seeded onto 96-well plates at $3x10^3$ cells per well in 100 μl suspensions in triplicate for each drug concentration and maintained in complete culture medium for 24 h. Then, the culture medium was changed with culture mediums containing different drug concentrations and maintained for 5 days. The culture medium was changed on the third day. Subsequently, cell viability was assessed using CCK-8 according to the manufacturer's instructions. Dose-response curves were plotted and the IC_{50}s were calculated using GraphPad Prism 8.

Detection of isocitrate dehydrogenase (IDH mutational status), 1p/19q codeletions, MGMTp methylation, telomerase reverse transcriptase (TERT) promoter mutation, and BRAFV600E mutation. DNA from cultured GWH04 cells and liquid nitrogen-frozen tumor tissues of the patient were extracted using the QIAamp DNA mini kit (Qiagen GmbH) according to the manufacturer's instructions. Next-generation sequencing was conducted to analyze the mutational status of IDH1/2, 1p/19q codeletions, TERT promoter mutation (C228T or C250T), and BRAF mutation (V600E). As pyrosequencing is a highly accurate method to analyze the changes at one or more CpG sites in the methylated sequence, the detection of the methylation status of the MGMT promoter region of GWH04 cells was conducted by Genetron (Beijing, China) using PyroMark Q24 sequencer (Qiagen China Co., Ltd.), which includes a complete software package for analyzing CpG site methylation and built-in controls for confirming the completeness of bisulfite processing.

Determination of glioma cell tumorigenicity. A total of 5 male and 5 female BALB/c athymic nude mice (age, 4-5 weeks; weight 19-21 g) were purchased from Hunan Silaike Jingda Laboratory Animal Co. (Changsha, China) and housed under specific pathogen-free conditions in a temperature- and humidity-controlled environment (room temperature, 20-26˚C; humidity, 40-60%; 12-h light/dark cycle; free access to food and water). All procedures in the animal experiments were approved (approval no. TJ-A20161206) by the Ethical Committee of Tongji Hospital, Tongji Medical College, Huazhong University of Science and Technology (Wuhan, China) and were performed in accordance with ARRIVE guidelines (https://arriveguidelines.org). The health and behavior of the mice were monitored five days once. First, GWH04 cells were harvested and injected subcutaneously into the right axilla of each mouse ($3x10^6$ cells/mouse) to test the tumorigenicity. On day 60, one mouse was found dead due to the tumor growth, and the other tumor-burdened nude mice were euthanized through intraperitoneal anesthesia of an overdose of pentobarbital sodium (150 mg/kg). The death of the mice was verified by the presentation of breath cessation and loss of heartbeat. Subsequently, the intracranial tumorigenic capacity was assessed in 5 female mice as this cell line was derived from a female patient. A short longitudinal incision was made in the scalp to expose the calvarium after anesthesia (pentobarbital sodium, intraperitoneal injection, 50 mg/kg). Then, a burr hole was made 0.5 mm posterior to the bregma and 1.5 mm to the right of the sagittal suture. A Hamilton syringe was introduced at a depth of 2 mm below the brain surface, and $5x10^5$ tumor cells (stably expressing luciferase) were slowly injected into the brain. When the mice began to lose weight and slow down actions, bioluminescence imaging indicated a definite lesion in 3 mice. On day 60, the three mice were euthanized as aforementioned and the brain tissues were surgically harvested, measured, fixed in 4% paraformaldehyde overnight at 25-28˚C, and embedded in paraffin. H&E and IHC staining (for GFAP, Nestin, EMA, EGFR, CD31 and Ki67) was conducted, and the results were compared with those for the respective stained patient tumor tissue.

Whole-exome sequencing (WES) of GWH04 cells. DNA from GWH04 cells (15th passage) was extracted as aforementioned for high-throughput next-generation sequencing. Library construction and whole-exome capture of genomic DNA were performed using the SureSelectXT Human All Exon V6 (Agilent Technologies, Inc.) and MGIEasy Exome Universal Library Prep Set-V1.0. The captured DNA was sequenced on an MGISEQ 2000 platform (BGI-Shenzhen, China) with 150-bp paired-end sequencing. The human genome data of

Hg19 from the UCSC Genome Browser (http://genome.ucsc.edu/) was used as a reference, and common mutated genes in GBM patients were analyzed in the cell line.

Chromosome karyotype analysis. Harvesting for metaphase chromosome preparations was performed by treating exponential growth phase cells with 0.25 μg/ml colchicine for 3 h. Then, enzymatic dispersal was performed with trypsin/EDTA, and the preparation was centrifuged at 1,000 x g for 6 min (25-28˚C). Preheated 0.075 mM KCl hypotonic solution was added for 15 min at 37˚C and fixed with 3:1 methanol-acetic acid (v:v; 25-28˚C; 1 min). The pellets were fixed twice at room temperature (25-28˚C) for 10 min, and 500 μl stationary liquid was added to resuspend the cells. Afterward, cell droplets were spotted onto clean microscope glass slides that had been soaked in iced water. The slides were immediately heated over an alcohol lamp for 2 sec to allow the chromosomes to spread out. Chromosome specimens were stained with Giemsa (cat. No. BA4219, Baso Diagnostics, Inc.) for 10 min at 25-28˚C according to the manufacturer's instructions, and the chromosome numbers of M phase cells were counted using an oil immersion lens (x100) under a microscope (Nikon Corporation). Karyotypes were determined by arranging all the photographed metaphases. The chromosomes were classified according to the International System for Human Cytogenetic Nomenclature (9).

Statistical analysis. All experiments were repeated at least twice with consistent results. The differences of the growth rate on day 5 of the cells, as well as the differences of the colony numbers and the relatively diameters of the cells (GWH04, U87 and GL15) were analyzed by one-way analysis of variance followed by a post hoc test (Dunnett's; Fig. 3A, C and D). All of these statistical analyses were performed using SPSS Statistics version 19 (IBM Corp.) and the graphs were drawn using GraphPad Prism 8 (GraphPad Software, Inc.). Alpha level was 0.05 in the present study. $P<0.05$ was considered to indicate a statistically significant difference. Dose-response curves of different drugs and the analysis of the corresponding IC_{50}s were also performed using GraphPad Prism 8 (Fig. 3E).

Results

Primary culture and identification of GWH04 cells. CT and MRI scans of the brain tumor and H&E staining of the paraffin-embedded tumor tissue of the patient are shown in Fig. 1. The histopathological diagnosis was GBM, based on the H&E staining, which showed numerous nuclear atypia, mitoses, and microvascular proliferation and different IHC staining items (Fig. S1). During the culture, GWH04 cells began to proliferate significantly faster in the 7th generation, and cell morphology was intended to be stable, as shown in passage 10 (P10) and passage 50 (P50), compared with passage 1 (P1) and 2 (P2) (Fig. 2A). Immunofluorescence staining was performed in the 10th generation, showing that GWH04 cells were positive for GFAP and Nestin expression (Fig. 2B). However, this GFAP expressed in GWH04 cells is markedly blurry even with longer exposure times when compared with GFAP expression in cultured cells digested from grade I-III gliomas (Fig. S2), despite these grade I-III glioma cells couldn't circumvent replicative senescence in the later culture. As GFAP is a marker of differentiated astrocytes and Nestin is a marker of neuroepithelial stem cells, GWH04 is a GBM cell line derived from dedifferentiated glial cells. A previous STR study of 482 different human tumor cell lines used in China showed that up to 96 cell lines were misidentified (10), and Nature research journals, AACR publications, and certain other scientific publishers currently require cell identification based on DNA analysis of the samples and cell lines used. In the present study, STR authentications of 20 locations (covering the 9 loci demanded by the ATCC) from the GWH04 cells and the corresponding tumor tissue were tested and a complete match was observed (Table I; Fig. 2C). Moreover, the STR profile differed from that of all cell lines available in different cell banks (http://cellresource.cn/str/default.aspx).

Genetic diagnoses of GWH04 cells. According to the 2016 World Health Organization Classification of Tumors of the Central Nervous System (11), genetic diagnosis is recommended to identify the mutational status of *IDH1/2*, *TERT* promoter, and BRAF, as well as 1p/19q co-deletions and MGMT promoter region methylation, which can help to predict prognosis and decide direct treatment options. In the present study, the GWH04 cells were harvested (P7) and the DNA was extracted for detection. The results were presented in Table II. The current consensus is that MGMT expression is inhibited by the methylation of MGMT promoter, and lower MGMT expression is associated with the TMZ-sensitivity. However, the CpG islands of the *MGMT* promoter were found to be unmethylated in this cell line, which results in the TMZ-resistance. Moreover, the *TERT* promoter region harbored a C228T mutation, which is frequently mutated and considered as a driver gene of GBM. Thus, the mutation status of Table II in this case indicates a poor prognosis of the patient and usually calls for a more aggressive treatment.

With the identification of these most commonly mutated genes associated with the formation of gliomas at GWH04 establishment, this cell line could be a useful tool in GBM research for the discovery of new antitumor compounds and the assessment of drug sensitivity, resistance, and toxicity biomarkers, as well as the identification of targeted agents showing clinical utility.

Cell proliferation and soft agar colony formation assays of GWH04 cells. The proliferation rate and tumorigenicity are basic features of primary cell lines, which are closely related to their popularity in cancer research. CCK-8 assays of GWH04 cells (the 10, 20 and 50th passage) were performed to detect the proliferation rates of different passages, which was compared with that of U87 and GL15 cells. During the first 2 days, GWH04 cells grew slower than U87 and GL15 cells, but this rate rapidly increased in the following 3 days, indicating that the growth of GWH04 cells is more density-dependent (Fig. 3A). The growth rates at the fifth day were of no significance among different passages of GWH04 cells and U87 cells (n=3; 10th GWH04 vs. U87, P=0.364; 20th GWH04 vs. U87, P=0.054; 50th GWH04 vs. U87, P=0.365), but were significantly faster of different passages of GWH04 cells than GL15 cells (n=3; 10th GWH04 vs. GL15, P<0.001;

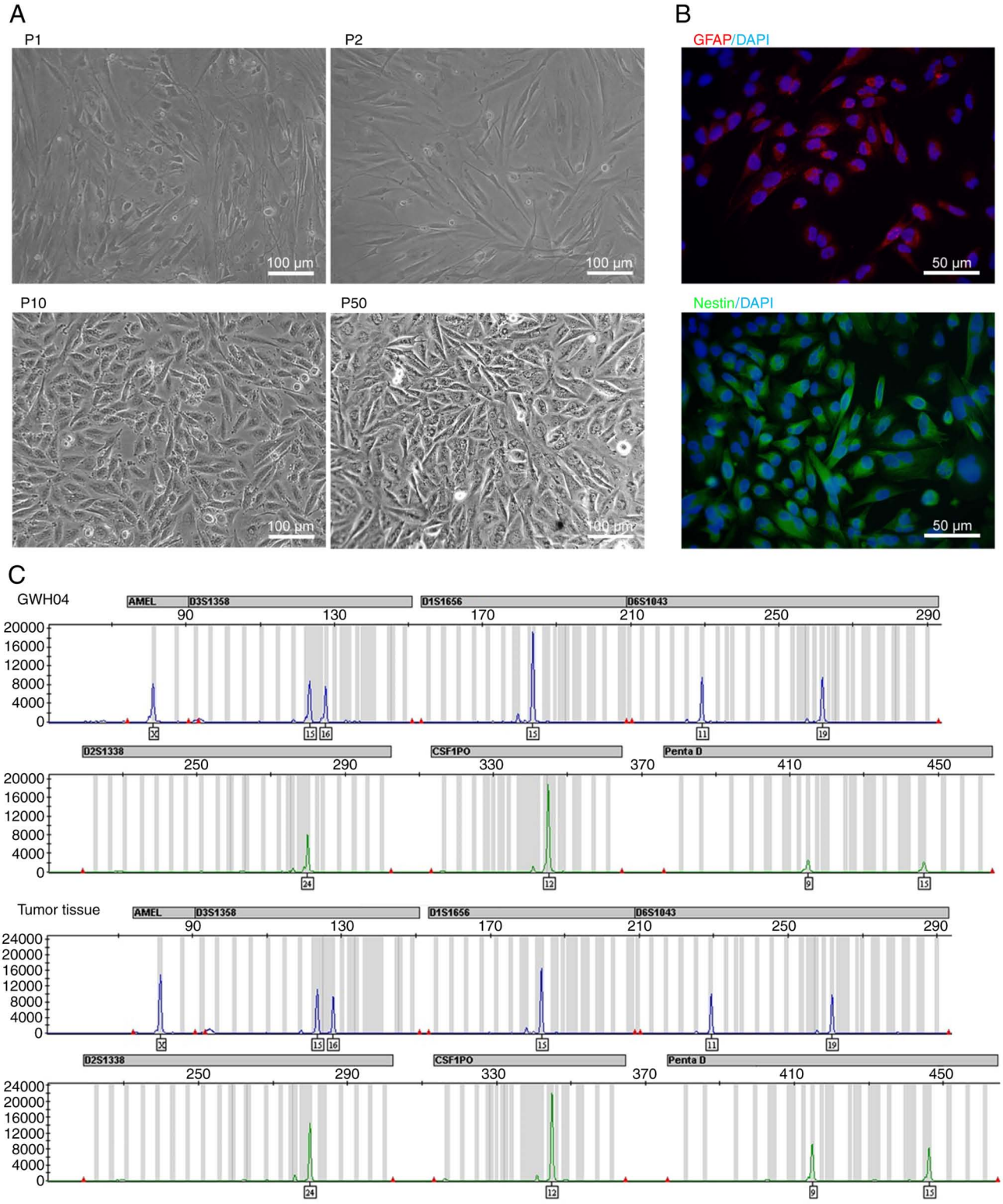

Figure 2. Bright field morphology, immunofluorescent staining and STR identification of GWH04. (A) Bright field morphology of GWH04 cells in the 1st, 2nd, 10th and 50th passage (P1, P2, P10, P50; scale bars, 100 μm). (B) The immunofluorescence staining of GFAP and Nestin. DAPI is a nuclear dye used as counterstain in immunofluorescence (magnification, x400; scale bars, 50 μm). (C) Part of STR loci identification map of GWH04 cells and the corresponding tumor tissue. STR, short-tandem repeat.

20th GWH04 vs. GL15, P<0.001; 50th GWH04 vs. GL15, P<0.001). Soft agar colony formation assays can preliminarily judge the tumorigenicity of cells *in vitro*. Thus, to examine the clone formation capacity of GWH04 cells, parallel experiments were conducted with U87 and GL15 cell lines. The assays showed that the colony formation number of GWH04 cells was slightly higher than that of U87 and GL15, but was not significantly different (Fig. 3B and C; GWH04 vs. U87, P=0.071; GWH04 vs. GL15, P=0.113). By contrast, the average diameter of GWH04 cells was significantly smaller than that of

Table I. Information of 20 STR loci of GWH04 cells and the corresponding tumor tissue.

STR loci	GWH04	Tumor tissue from patient
Amelogenin	X, X	X, X
D3S1358	15, 16	15, 16
D1S1656	15, 15	15, 15
D6S1043	11, 19	11, 19
D13S317	9, 9	9, 9
PentaE	12, 18	12, 18
D16S539	10, 12	10, 12
D2S1338	24, 24	24, 24
CSF1PO	12, 12	12, 12
PentaD	9, 15	9, 15
TH01	7, 9	7, 9
vWA	14, 17	14, 17
D21S11	30, 30	30, 30
D7S820	11,12	11,12
D5S818	12, 13	12, 13
TPOX	8, 9	8, 9
D8S1179	12, 13	12, 13
D12S391	22, 23	22, 23
D19S433	14, 14	14, 14
FGA	22, 23	22, 23

STR, short-tandem repeat.

Table II. Results of WHO recommended genetic testing for gliomas.

Tested items	Results
MGMT promoter methylation	Unmethylated
1p deletion	Intact
19q deletion	Deleted
IDH1 R132 mutation	No mutation
IDH2 R172 mutation	No mutation
TERT promoter C228T mutation	No mutation
TERT promoter C250T mutation	Mutated
BRAF V600E mutation	No mutation

MGMT, O6-methylguanine-DNA methyltransferase; TERT, telomerase reverse transcriptase; IDH, isocitrate dehydrogenase.

U87 and GL15 cells (Fig. 3B and D; GWH04 vs. U87, P=0.004; GWH04 vs. GL15, P<0.001), indicating that this newly established cell line possesses a higher clone formation capacity, but a lower proliferation rate of anchorage-independent growth than U87 and GL15 cells.

IC_{50} tests of different drugs. TMZ is the first line chemotherapy strategy for GBM treatment in recent decades (12), and CCNU has been demonstrated to provide a benefit for GBM patients in terms of both progression-free survival and overall survival, despite increased adverse events (13,14). Numerous patients with advanced GBM may have treatment with bevacizumab, irinotecan, etoposide (VP-16), 5-Fu, and cisplatin as the second line or the rescue treatment strategy, even though not all pre-clinical studies have presented satisfactory therapeutic results (15-18). As the amplification and activation of EGFR are the most commonly RTK aberrations in GBMs (19), and GWH04 cells possess TERT promoter mutation and BRCA1 mutation (presented below), gefitinib (EGFR inhibitor), BIBR1532 (telomerase inhibitor) and Olaparib (PARP inhibitor, which shows standalone activity against BRCA1-deficient breast cancer cell lines) were also selected.

In the present study, GWH04, U87 and GL15 cells were simultaneously exposed to TMZ, CCNU, SN-38 (an active metabolite of irinotecan), VP-16, 5-Fu, oxaliplatin, gefitinib, BIBR1532 and Olaparib. The growth rate inhibition metrics with each condition after 5 days of drug exposure and fitted dose-response curves of different drugs, as well as the IC_{50}s, are presented in Fig. 3E. When compared with U87 and GL15, GWH04 appears to be more sensitively to VP-16, 5-Fu, oxaliplatin and olaparib *in vitro* (Fig. 3E). The IC_{50} of GWH04 cells is 858.2 μM treated with TMZ *in vitro*, which indicates definite TMZ-resistance when compared with T98G cells (800 μM) (20). Furthermore, the unmethylated promoter region of *MGMT* also indicated resistance to TMZ treatment. Thus, GWH04 is a primary TMZ-resistant cell line.

Subcutaneous and intracranial tumorigenicity. Not every cell line can form xenograft tumors in nude mice; for example, U251 and U87 cells are tumorigenic, but HS683 and A172 are not (7,8). Indeed, in a study of 34 randomly selected human glioma cell lines, only 19 (56%) were able to generate tumors in immunocompromised mice (7). Combined with the observation that only ~10% of GBMs will generate permanent/immortal cell lines *in vitro* when cultured in standard medium (7), it is clear that tumorigenicity in immunocompromised mice and immortalization *in vitro* are distinct phenotypes.

To determine whether GWH04 cells possess tumorigenic capacity *in vivo*, subcutaneous and intracranial injection were conducted. The subcutaneous tumor-burdened nude mice and the harvested tumors on day 60 were presented in Fig. 4A, which confirmed the well tumorigenic capacity of this cell line. For intracranial injected mice, when obviously poor general conditions were detected, the bioluminescence imaging indicated a definite lesion in 3 mice. Then, the mice were euthanized, the brain tissue was surgically harvested and analyzed by H&E and IHC staining (Fig. 4B and C). Both mouse intracranial xenografts and primary tumor tissues of the patient positively expressed GFAP, Nestin, EMA, EGFR, Ki67 and CD31 (Fig. 4C). Ki67 expression indicated that the proliferation status was markedly more active in the mouse intracranial xenograft than in the primary tumor of the patient (Fig. 4C), probably owing to the fact that *in vitro* culture enriched the cells with stronger proliferative ability. The histological features of microvascular hyperplasia and palisade necrosis were of highly consistence between the GBM tissue of the patient and the tumorigenic tissue in nude mice (Fig. 4C). These results indicated the culture system faithfully recapitulated and maintained the expression status of the

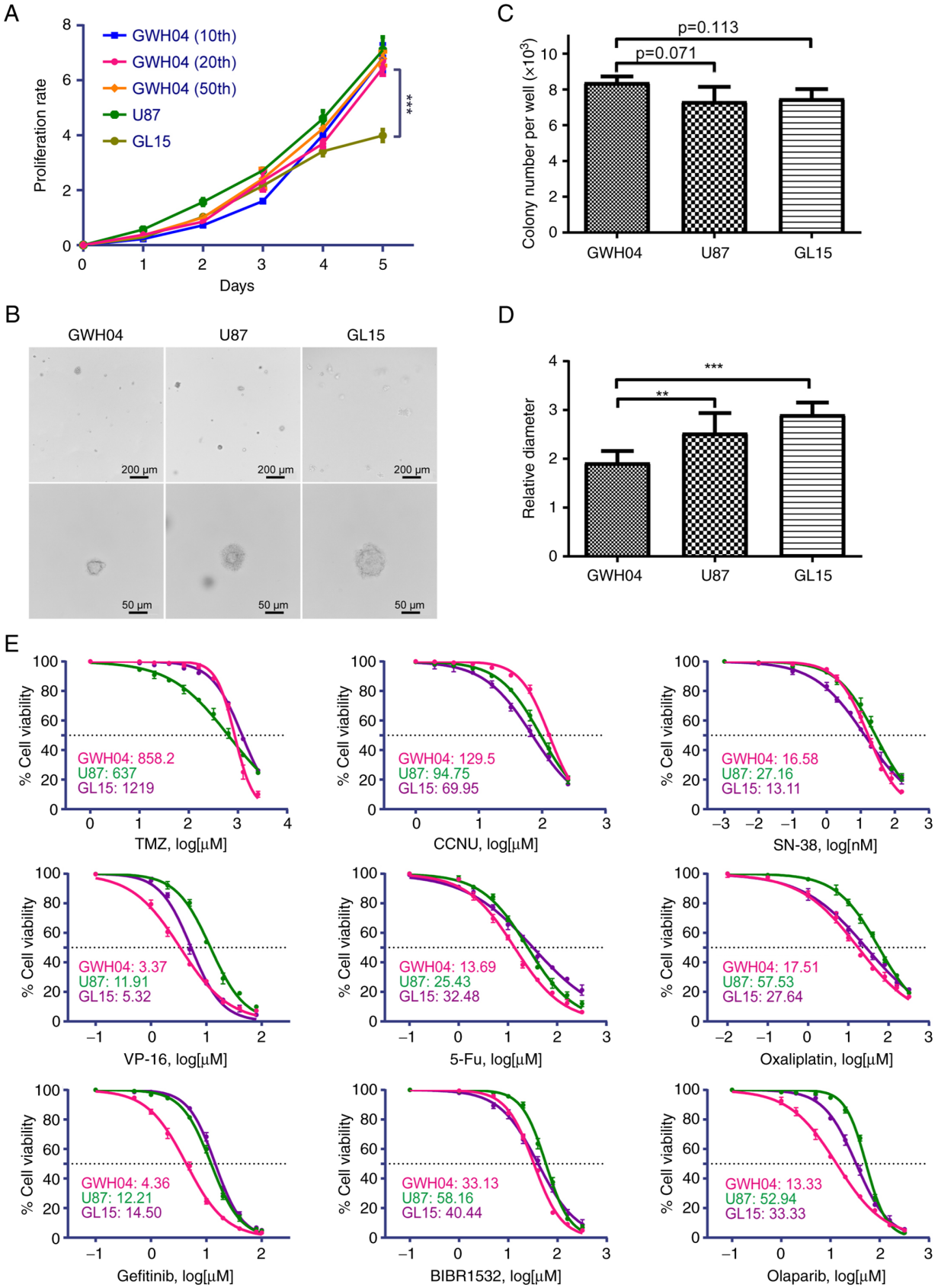

Figure 3. Proliferation rate, anchorage-independent growth capacity and chemotherapy sensitivity of several drugs of GWH04. (A) Analysis of proliferation rates with Cell Counting Kit-8 in GWH04 (the 10, 20 and 50th passages), U87 and GL15 cells. (B) Anchorage-independent proliferation with colony formation assays of GWH04, U87 and GL15 cells. Representative images of soft agar colonies in each cell line are presented (Scale bars, upper panel, 200 μm; lower panel, 50 μm). (C) Quantitative analysis of colony numbers per well of each group (n=3 independent wells per cell line; data represent the mean ± SD of three independent experiments). (D) Quantitative analysis of diameters of 10 different clones showed that GWH04 cells formed significantly smaller clones than that of U87 and GL15 cells (n=10 biologically independent colonies per cell line). **P<0.01 and ***P<0.001. (E) The corresponding dose-response curves of GWH04, U87 and GL15 cells exposed to increasing concentrations of different drugs, and the IC_{50s} of each drug were presented. IC_{50}, half maximal inhibitory concentration.

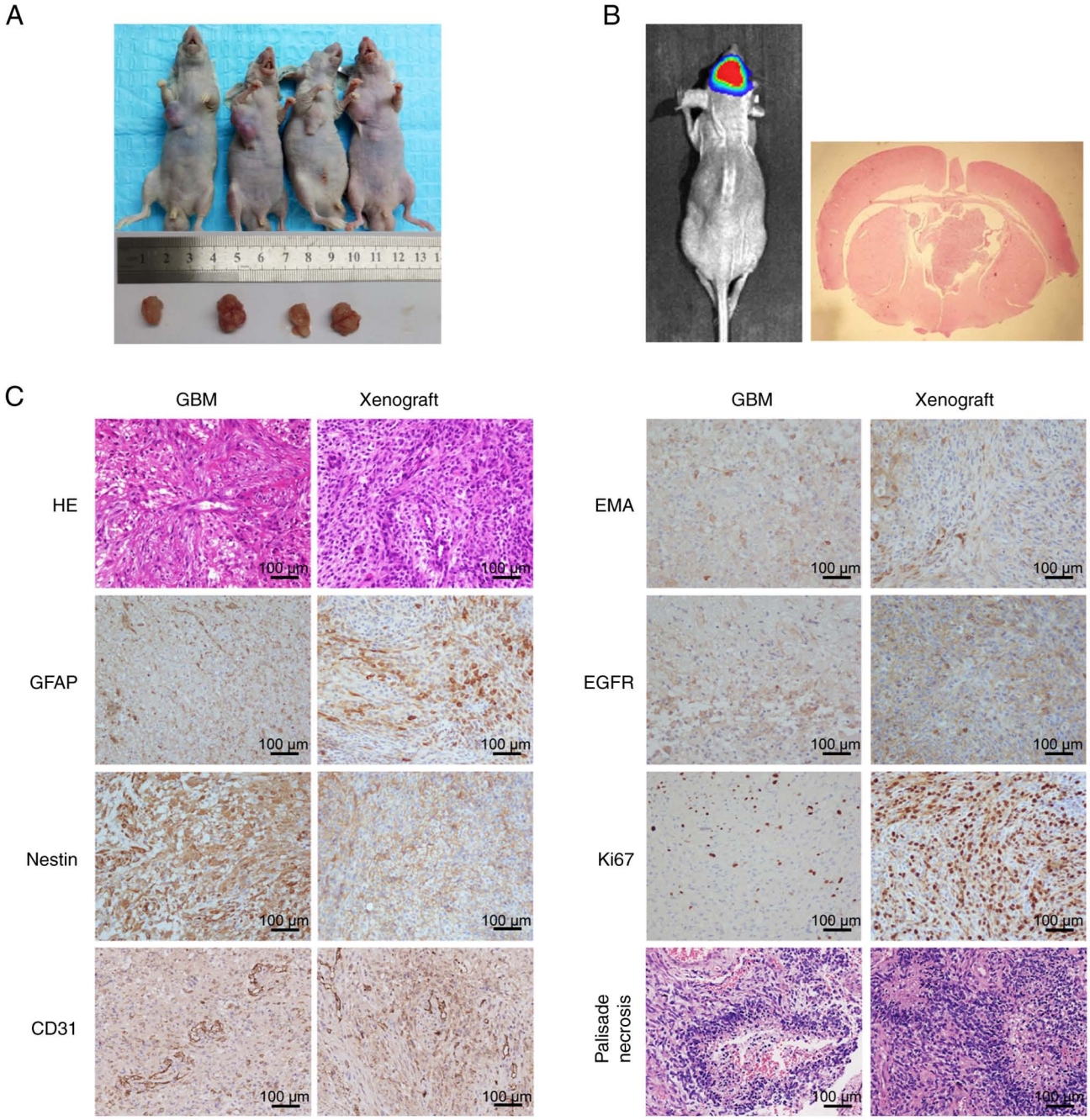

Figure 4. Tumorigenic capacity of GWH04 cells. (A) Images of nude mice bearing GWH04 subcutaneous xenografts, and the harvested tumors were presented in the lower panel. (B) Bioluminescence imaging and H&E staining of the mouse brain tissue obtained after 60 days post-implantation. (C) Tumor tissues from nude mice and the primary GBM tissue of the patient were sectioned and stained for HE and the expression of GFAP, Nestin, EMA, EGFR Ki67 and CD31. Representative images are shown (Scale bar, 100 μm). GBM, glioblastoma multiforme; GFAP, glial fibrillary acidic protein.

primary tumor and also indicate the substantial tumorigenicity of GWH04 cells. In conclusion, GWH04 cell line will be a useful tool for both *in vitro* and *in vivo* GBM research.

Mutated genes associated with tumorigenicity in GWH04 cells. Apart from the several genetic factors recommended for analysis to support diagnosis and treatment, numerous other gene mutations are firmly related to the occurrence and development of gliomas. Ishii *et al* (7) studied tumor suppressor genes, namely *TP53*, *p16*, *p14ARF*, and *PTEN*, in 34 randomly selected human glioma cells and found that mutations and deletions occurred at the following frequencies: *TP53* (76.5%), *p14ARF* (64.7%), *p16* (64.7%) and *PTEN* (73.5%). Another study demonstrated that ~86% of GBM samples harbor at least one genetic event in the core RTK/PI3K pathway, such as in *EGFR*, *ERBB2*, *PDGFRA*, or *MET* (21). To investigate the mutational status of these important genes and other associated genes in GWH04 cells, WES was performed. GWH04 cells were found to possess mutated *TP53*, *PTEN*, *PDGFRA*, *ERBB2*, *BRCA1*, *NF1*, and *MLH1*, and wild-type *CDKN2A*, *PIK3R1*, *PIK3CA*, *Rb1* and *MET*. The sequencing and gene mutation data are shown in Table III.

Chromosome karyotype of GWH04 cells. In addition to heterogeneity in the biological and molecular features of

Table III. List of certain mutated genes based on whole-exome sequencing of GWH04 cells.

Gene	Location	Mutation type	Transcript
TP53	17p13.1	missense_variant	ENST00000269305:p.Tyr205Cys/c.614A>G
PTEN	10q23.31	stop_gain	ENST00000371953:p.Tyr315*/c.945T>A
PDGFRA	4q12	missense_variant	ENST00000257290:p.Ser478Pro/c.1432T>C
ERBB2	17q12	missense_variant	ENST00000269571:p.Ser423Gly/c.1267A>G
BRCA1	17q21.31	missense_variant	ENST00000471181:p.Glu1038Gly/c.3113A>G
NF1	17q11.2	stop_lost	ENST00000471572:p.Ter640Argext*?/c.1918T>C
MLH1	3p22.2	missense_variant	ENST00000231790:p.Val384Asp/c.1151T>A

refers to the last changed amino acid; ext? refers to the extension to an unknown amino acid.

GBM, chromosomal instability (CIN) is a frequently occurring event in cancer that involves numerical abnormalities of chromosomes and large-scale structural alterations. Previous studies have demonstrated that GBM cell lines have hyperdiploid karyotypes and exhibit glioma-specific chromosomal abnormalities, such as gain of chromosome 7 and loss of chromosome 10 (4,9). The range of possible chromosome numbers of certain GBM cell lines based on previous studies was compiled and presented in Table IV.

To determine whether GWH04 cells had CIN, the 10th passage cells were harvested for G-banding karyotype analysis and G-banding metaphase images were obtained. The chromosomal number ranged from 61 to 125 while counting 40 karyotypes, and the first and third quartiles were 82 and 86, respectively (Fig. 5A). Chromosome karyotype pairing showed that extra copies of different chromosomes were rather common, and aberrantly structured chromosomes presented with two unknown chromosomes in one karyotype analysis (Fig. 5B). Considering that reported glioma cell lines are all hyperdiploid (5,9,22,23), it was concluded that this is a common phenomenon in glioma and glioma cell lines. In addition to chromosome number abnormalities, chromosomal structural abnormalities, such as broken chromosomes, double centromere chromosomes, homogeneous staining regions (HSR), and double microbodies, were presented in other karyotype analyses of GWH04 cells (Fig. 5C). These changes in the overall chromosomal configuration expand our understanding of the CIN and heterogeneity of tumor cells.

Subclone analysis. The karyotype analysis of GWH04 cells at the 10th passage demonstrated the prevalence of chromosome number abnormalities and chromosomal structural abnormalities. To understand in an improved way the dynamic CIN of GWH04 cells, monoclonal culture derived from these cells and karyotype analyses of three subclones (subclone 1.4, 1.5, and 3.17) were conducted and compared. The chromosome numbers of the three subclones were not exactly the same, with a narrow range of fluctuations and more common dicentric chromosomes compared with results based on GWH04 cells. The chromosome numbers of 40 metaphase karyotypes from subclones 1.4, 1.5, and 3.17 cells exhibited ranges of 59-83, 70-87, and 55-91, with 7.5% (3/40), 40% (16/40), and 20% (8/40) positive for dicentric chromosomes, respectively (Fig. 5D). As genetic and genomic aberrations are the primary cause of cancer, chromosome mis-segregation leads to aneuploidy, and aberrant chromosomes provide cancer cells with a mechanism to lose tumor suppressor loci and gain extra copies of oncogenes, which will definitely increase the mutation rates and malignancy of offspring cells.

Table IV. Abnormal chromosome numbers in glioma cell lines from previous studies.

Cell line	Number of chromosomes	Number of karyotyped cells	(Refs.)
GL15	75-90	20	(9)
GL22	56-73	10	(9)
K308	54-108	100	(22)
ANGM-CSS	88-91	-	(23)
SHG140	55	1	(24)
LN18	70-80	-	(5)

Discussion

Cell culture and cell lines are the fundamental and most powerful tools in cancer research. They are often used in cancer biology studies and for the discovery of new anti-tumor compounds, drug sensitivity and resistance, toxicity biomarkers, and targeted agents showing clinical utility. However, the accumulation of genetic aberrations in cancer cell lines often occurs with increasing passage numbers, making it impossible for numerous preclinical studies to translate into clinical application. Therefore, establishing new primary cancer cell lines derived from primary tumor tissues is of crucial importance for different cancer research studies.

In recent years, primary culture conditions for GBM have mainly been high-glucose DMEM or RPMI-1640 supplemented with 10% FBS for 2D adhesion culture and serum-free culture medium (neurobasal medium + B27 + EGF + FGF) for 3D suspension sphere culture, as the latter maintains more stem cell features (24-26). Different culture conditions were selected according to different study goals.

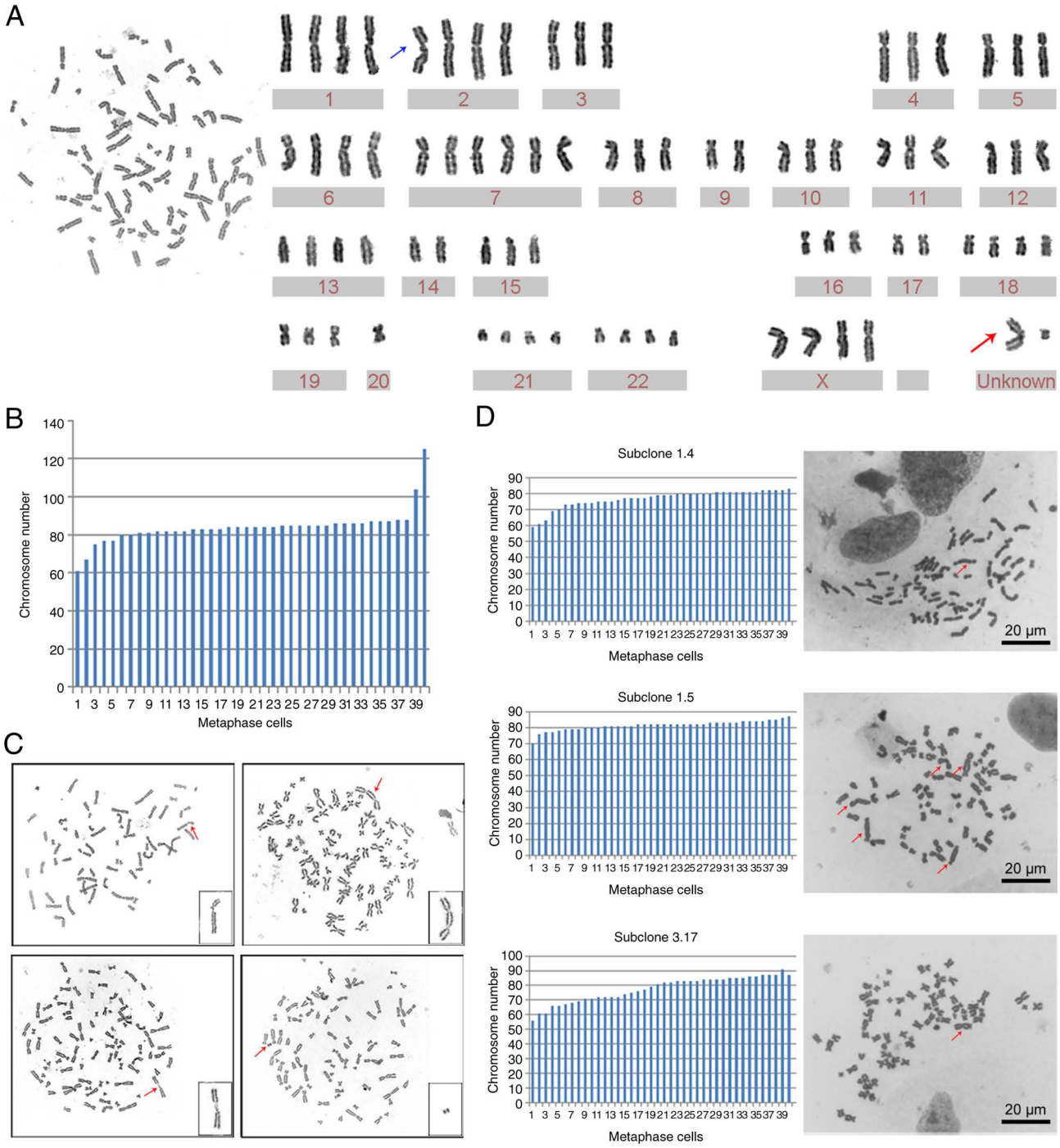

Figure 5. Karyotype analysis of GWH04 cell line and chromosomal instability presented in three subclones of GWH04 cells. (A) Chromosome karyotype pairing in one karyotype analysis showed extra copies of different chromosome, one broken chromosome (blue arrow) and two unknown chromosomes (red arrow). (B) The chromosomal numbers of 40 different G-banding metaphase cells. (C) Several other karyotype analyses of GWH04 cells demonstrated chromosomal structural abnormalities. Arrows indicated abnormal chromosomes (broken chromosome, double centromere chromosome, homogeneous staining region and double microbodies). (D) Chromosome number and frequently occurred double centromeric chromosome in three different monoclones (subclone 1.4, subclone 1.5 and subclone 3.17) of GWH04 cell line.

Compared with sphere culture cell lines, adherent cultures are easy to manipulate for common experimental purposes, such as transfection, transduction and drug screening. Adherent tumor cell lines are also amenable to growth in sphere cultures and are commonly switched to sphere cultures for specific assays. In the present study, culture from 10 GBM tissues of different patients was conducted in the same culture medium (high-glucose DMEM + 10% FBS), but only GWH04 cells from patient 4 could circumvent replicative senescence and acquire the ability to sustain unlimited proliferation in this culture medium. As the genetic backgrounds of different GBMs are not determined when establishing primary cultures from fresh patient-derived tissues, high efficiencies can result from culturing samples with various media conditions that differ in their combinations of growth factors.

For the identification of GWH04 cells, immunofluorescence staining of GFAP and Nestin was conducted. GFAP, a glial fibrillary acidic protein, is a marker of astrocyte activation. Although GFAP can be readily detected in most astrocytic glioma and GBM cells, only the most morphologically differentiated cells express it, whereas more primitive and anaplastic cells do not (4). Nestin, an intermediate filament protein that is specifically expressed in neuroepithelial stem cells, is a marker of neural stem cells. It is normally expressed in the neuroepithelium during the early stage of embryonic development. For normal brain tissue and normal astrocytic cells, Nestin expression is negative. In the present study, immunofluorescence staining showed clear Nestin expression with a distinct sense of cytoskeleton fibers, which indicated firm derivation from tumor cells, whereas the GFAP expression pattern was blurry even with longer exposure times when compared with GFAP expression in cultured cells digested from grade I-III gliomas (stained under the same conditions). However, this did not affect protein expression in the mouse intracranial xenografts of this cell line. Bigner *et al* (4) showed that only two of the 15 GBM cell lines (U251 MG and U251 MG sp) yielded positive immunofluorescent reactions for GFAP, and another study showed that, in the early passages, ~30% of GL15 and 40% of GL22 cells exhibit GFAP immunoreactivity in the fibrils of the cytoplasm (9). In conclusion, Nestin staining is more reliable than GFAP staining when identifying GBM-derived tumor cells.

TP53 is a typical tumor suppressor gene associated with several biological processes, such as DNA damage repair, apoptosis and proliferation (27). Indeed, among all genes in human cancer cell genomes examined to date, *TP53* is the most frequently mutated gene and is mutated in almost one-third of all human tumors (28). Ishii *et al* (7) confirmed preliminary observations that the incidence of TP53 mutations is markedly higher in GBM cell lines (>75%) than in gliomas (25-35%). Moreover, as *TERT* encodes a highly specialized reverse transcriptase, which adds hexamer repeats to the 3'-end of chromosomes (29), somatic mutations in the *TERT* promoter region (C228T or C250T) increase telomerase activity leading to preservation of telomeres, thereby allowing tumors to avoid the induction of senescence (30). As GWH04 cells possess mutations in both TP53 and *TERT* promoter region (C228T), it is reasonable to consider that the accommodation of GWH04 cells both *in vitro* and *in vivo* may result from the combination of different mutations. With the continuous optimization of current technology and culture conditions, primary culture is expected to improve in the future.

Genome instability is a common characteristic of tumor cells. Notably, GWH04 cells were found to have chromosome number abnormalities and structural abnormalities. Karyotype analysis of several subclones illustrated the dynamic chromosome instability of these cells. The increased tolerance to chromosomal segregation errors could contribute to the association between hyperploidy and genomic complexity, and may reflect the progressive adaptation of self-renewing cells to the microenvironment *in vivo* and their culture conditions *in vitro* (31). When considering chromosomal structural abnormalities, double microbodies and HSR were presented in certain G-banding metaphase images. It has been reported that double microbodies are large extracellular DNA (ecDNA), and ecDNA has been demonstrated to be rather common in GBM and to be associated with oncogene amplification and targeted therapy resistance (32-34). HSR was also reported to be associated with amplified oncogenes, such as MYC, EGFR and ERBB2 (35). Therefore, exploring relevant therapy from the perspective of aneuploidy and chromosomal abnormalities, may be effective for treating GBM.

Given the common use of several cell lines to illustrate the function and contribution of a single molecule and/or mutation to cancer, it is of great importance to learn more about the mutation background of each cell line. If a study is based on several cell lines with similar mutational landscapes and the cell lines are from early passages with a high similarity to the primary tumor, it is expected that the transition time from preclinical to clinical research will be shortened. As GWH04 cells are presented with complete genetic information and cell biological characteristics, readers could have a deeper insight of it. To date, this cell line has demonstrated to be easy to manipulate for common experimental purposes with strong stability in various experimental studies, such as transfection, transduction and drug screening *in vitro*, as well as to form xenografts in nude mice *in vivo*. Any researcher interested in GBM study can obtain this cell line from either institution of BRICS or CCTCC. This will facilitate the exploration of molecular mechanisms and the screening and evaluation of antitumor drugs in GBM studies.

Acknowledgements

The authors would like to thank Professors Zhang Songling and Yu Changjie at the BRICS for the identification of this cell line.

Funding

The present study was supported by the National Natural Science Foundation of China (grant nos. 81874086).

Availability of data and materials

The datasets used and/or analyzed during the current study are available from the corresponding author on reasonable request. The WES-seq dataset generated and/or analyzed during the current study is available in the NCBI repository (https://www.ncbi.nlm.nih.gov/bioproject/PRJNA806683).

Authors' contributions

FM and DG discussed the project and designed the research. FM and BW confirm the authenticity of all the raw data. FC and FM put forward the ideas of this article, conducted the primary culture and wrote the manuscript. BW revised the manuscript. FC and XW performed the karyotype analysis and animal experiments. YL and PP conducted the data acquisition and analysis from CCK-8 and soft agar colony formation assays. CH collected the clinical samples and conducted the follow-up record collections. SX and BW performed the pathological examination of tumor tissue and xenografts. All authors read and approved the final manuscript.

Ethics approval and consent to participate

Detailed information was given to the relatives of the patient and informed consent was provided prior to surgery. All samples were obtained from the Department of Neurosurgery, Tongji Hospital, Huazhong University of Science and Technology (Wuhan, China) after written informed consent was obtained and according to the protocol approved (approval no. TJ-IBR20210119) by the Research Ethics Committee of Tongji Hospital, Tongji Medical College, Huazhong University of Science and Technology. All procedures involving human samples were in accordance with the 1964 Helsinki Declaration and its later amendments or comparable ethical standards.

All procedures in the animal experiments were approved (approval no. TJ-A20161206) by the Ethical Committee of Tongji Hospital, Tongji Medical College, Huazhong University of Science and Technology and were performed in accordance with ARRIVE guidelines (36) (https://arriveguidelines.org).

Patient consent for publication

The relatives of the patient provided written informed consent before the surgery for the study of this case and for the publication of the data and accompanying images. The right of the patient to anonymity and privacy was fully respected.

Competing interests

The authors declare that they have no competing interests.

References

1. Wen PY and Reardon DA: Neuro-oncology in 2015: Progress in glioma diagnosis, classification and treatment. Nat Rev Neurol 12: 69-70, 2016.
2. Noushmehr H, Weisenberger DJ, Diefes K, Phillips HS, Pujara K, Berman BP, Pan F, Pelloski CE, Sulman EP, Bhat KP, *et al*: Identification of a CpG island methylator phenotype that defines a distinct subgroup of glioma. Cancer Cell 17: 510-522, 2010.
3. Allen M, Bjerke M, Edlund H, Nelander S and Westermark B: Origin of the U87MG glioma cell line: Good news and bad news. Sci Transl Med 8: 354re3, 2016.
4. Bigner DD, Bigner SH, Pontén J, Westermark B, Mahaley MS, Ruoslahti E, Herschman H, Eng LF and Wikstrand CJ: Heterogeneity of genotypic and phenotypic characteristics of fifteen permanent cell lines derived from human gliomas. J Neuropathol Exp Neurol 40: 201-229, 1981.
5. Diserens AC, de Tribolet N, Martin-Achard A, Gaide AC, Schnegg JF and Carrel S: Characterization of an established human malignant glioma cell line: LN-18. Acta Neuropathol 53: 21-28, 1981.
6. Van Meir E, Sawamura Y, Diserens AC, Hamou MF and de Tribolet N: Human glioblastoma cells release interleukin 6 in vivo and in vitro. Cancer Res 50: 6683-6688, 1990.
7. Ishii N, Maier D, Merlo A, Tada M, Sawamura Y, Diserens AC and Van Meir EG: Frequent co-alterations of TP53, p16/CDKN2A, p14ARF, PTEN tumor suppressor genes in human glioma cell lines. Brain Pathol 9: 469-479, 1999.
8. Van Meir EG, Kikuchi T, Tada M, Li H, Diserens AC, Wojcik BE, Huang HJ, Friedmann T, de Tribolet N and Cavenee WK: Analysis of the p53 gene and its expression in human glioblastoma cells. Cancer Res 54: 649-652, 1994.
9. Bocchini V, Casalone R, Collini P, Rebel G and Lo Curto F: Changes in glial fibrillary acidic protein and karyotype during culturing of two cell lines established from human glioblastoma multiforme. Cell Tissue Res 265: 73-81, 1991.
10. Bian X, Yang Z, Feng H, Sun H and Liu Y: A combination of species identification and STR profiling identifies cross-contaminated cells from 482 human tumor cell lines. Sci Rep 7: 9774, 2017.
11. Louis DN, Perry A, Reifenberger G, von Deimling A, Figarella-Branger D, Cavenee WK, Ohgaki H, Wiestler OD, Kleihues P and Ellison DW: The 2016 World Health Organization classification of tumors of the central nervous system: A summary. Acta Neuropathol 131: 803-820, 2016.
12. Stupp R, Hegi ME, Mason WP, van den Bent MJ, Taphoorn MJ, Janzer RC, Ludwin SK, Allgeier A, Fisher B, Belanger K, *et al*: Effects of radiotherapy with concomitant and adjuvant temozolomide versus radiotherapy alone on survival in glioblastoma in a randomised phase III study: 5-Year analysis of the EORTC-NCIC trial. Lancet Oncol 10: 459-466, 2009.
13. Herrlinger U, Tzaridis T, Mack F, Steinbach JP, Schlegel U, Sabel M, Hau P, Kortmann RD, Krex D, Grauer O, *et al*: Lomustine-temozolomide combination therapy versus standard temozolomide therapy in patients with newly diagnosed glioblas-0toma with methylated MGMT promoter (CeTeG/NOA-09): A randomised, open-label, phase 3 trial. Lancet 393: 678-688, 2019.
14. Killock D: Lomustine-temozolomide combination efficacious in newly diagnosed glioblastoma. Nat Rev Clin Oncol 16: 273, 2019.
15. Wick W, Gorlia T, Bendszus M, Taphoorn M, Sahm F, Harting I, Brandes AA, Taal W, Domont J, Idbaih A, *et al*: Lomustine and bevacizumab in progressive glioblastoma. New Engl J Med 377: 1954-1963, 2017.
16. Friedman HS, Prados MD, Wen PY, Mikkelsen T, Schiff D, Abrey LE, Yung WK, Paleologos N, Nicholas MK, Jensen R, *et al*: Bevacizumab alone and in combination with irinotecan in recurrent glioblastoma. J Clin Oncol 27: 4733-4740, 2009.
17. Jeremic B, Grujicic D, Jevremovic S, Stanisavljevic B, Milojevic L, Djuric L and Mijatovic L: Carboplatin and etoposide chemotherapy regimen for recurrent malignant glioma: A phase II study. J Clin Oncol 10: 1074-1077, 1992.
18. Buckner JC, Ballman KV, Michalak JC, Burton GV, Cascino TL, Schomberg PJ, Hawkins RB, Scheithauer BW, Sandler HM, Marks RS, *et al*: Phase III trial of carmustine and cisplatin compared with carmustine alone and standard radiation therapy or accelerated radiation therapy in patients with glioblastoma multiforme: North central cancer treatment group 93-72-52 and southwest oncology group 9503 trials. J Clin Oncol 24: 3871-3879, 2006.
19. Snuderl M, Fazlollahi L, Le LP, Nitta M, Zhelyazkova BH, Davidson CJ, Akhavanfard S, Cahill DP, Aldape KD, Betensky RA, *et al*: Mosaic amplification of multiple receptor tyrosine kinase genes in glioblastoma. Cancer Cell 20: 810-817, 2011.
20. Yi GZ, Huang G, Guo M, Zhang X, Wang H, Deng S, Li Y, Xiang W, Chen Z, Pan J, *et al*: Acquired temozolomide resistance in MGMT-deficient glioblastoma cells is associated with regulation of DNA repair by DHC2. Brain 142: 2352-2366, 2019.
21. McLendon R, Friedman A, Bigner D, Van Meir EG, Brat DJ, Mastrogianakis GM, Olson JJ, Mikkelsen T, Lehman N, Aldape K, *et al*: Comprehensive genomic characterization defines human glioblastoma genes and core pathways. Nature 455: 1061-1068, 2008.
22. Yao PS, Kang DZ, Wang XF, Lin RY and Ye ZC: Cell-density-dependent manifestation of partial characteristics for neuronal precursors in a newly established human gliosarcoma cell line. In Vitro Cell Dev Biol Anim 51: 345-352, 2015.
23. Notarangelo A, Trombetta D, D'Angelo V, Parrella P, Palumbo O, Storlazzi CT, Impera L, Muscarella LA, La Torre A, Affuso A, *et al*: Establishment and genetic characterization of ANGM-CSS, a novel, immortal cell line derived from a human glioblastoma multiforme. Int J Oncol 44: 717-724, 2014.
24. Li Y, Sun T, Chen Z, Shao Y, Huang Y and Zhou Y: Characterization of a new human astrocytoma cell line SHG140: Cell proliferation, cell phenotype, karyotype, STR markers and tumorigenicity analysis. J Cancer 12: 371-378, 2021.
25. Li Y, Wang H, Sun T, Chen J, Guo L, Shen H, Du Z and Zhou Y: Biological characteristics of a new human glioma cell line transformed into A2B5(+) stem cells. Mol Cancer 14: 75, 2015.
26. Man J, Yu X, Huang H, Zhou W, Xiang C, Huang H, Miele L, Liu Z, Bebek G, Bao S and Yu JS: Hypoxic induction of vasorin regulates notch1 turnover to maintain glioma stem-like cells. Cell Stem Cell 22: 104-118.e6, 2018.
27. Aubrey BJ, Strasser A and Kelly GL: Tumor-suppressor functions of the TP53 pathway. Cold Spring Harb Perspect Med 6: a026062, 2016.
28. Bouaoun L, Sonkin D, Ardin M, Hollstein M, Byrnes G, Zavadil J and Olivier M: TP53 variations in human cancers: New lessons from the IARC TP53 database and genomics data. Hum Mutat 37: 865-876, 2016.

29. Cesare AJ and Reddel RR: Alternative lengthening of telomeres: Models, mechanisms and implications. Nat Rev Genet 11: 319-330, 2010.
30. Labussière M, Di Stefano AL, Gleize V, Boisselier B, Giry M, Mangesius S, Bruno A, Paterra R, Marie Y, Rahimian A, *et al*: TERT promoter mutations in gliomas, genetic associations and clinico-pathological correlations. Br J Cancer 111: 2024-2032, 2014.
31. Dewhurst SM, McGranahan N, Burrell RA, Rowan AJ, Grönroos E, Endesfelder D, Joshi T, Mouradov D, Gibbs P, Ward RL, *et al*: Tolerance of whole-genome doubling propagates chromosomal instability and accelerates cancer genome evolution. Cancer Discov 4: 175-185, 2014.
32. Kim H, Nguyen NP, Turner K, Wu S, Gujar AD, Luebeck J, Liu J, Deshpande V, Rajkumar U, Namburi S, *et al*: Extrachromosomal DNA is associated with oncogene amplification and poor outcome across multiple cancers. Nat Genet 52: 891-897, 2020.
33. Koche RP, Rodriguez-Fos E, Helmsauer K, Burkert M, MacArthur IC, Maag J, Chamorro R, Munoz-Perez N, Puiggròs M, Dorado Garcia H, *et al*: Extrachromosomal circular DNA drives oncogenic genome remodeling in neuroblastoma. Nat Genet 52: 29-34, 2020.
34. Nathanson DA, Gini B, Mottahedeh J, Visnyei K, Koga T, Gomez G, Eskin A, Hwang K, Wang J, Masui K, *et al*: Targeted therapy resistance mediated by dynamic regulation of extrachromosomal mutant EGFR DNA. Science 343: 72-76, 2014.
35. Turner KM, Deshpande V, Beyter D, Koga T, Rusert J, Lee C, Li B, Arden K, Ren B, Nathanson DA, *et al*: Extrachromosomal oncogene amplification drives tumour evolution and genetic heterogeneity. Nature 543: 122-125, 2017.
36. Percie du Sert N, Ahluwalia A, Alam S, Avey MT, Baker M, Browne WJ, Clark A, Cuthill IC, Dirnagl U, Emerson M, *et al*: Reporting animal research: Explanation and elaboration for the ARRIVE guidelines 2.0. PLoS Biol 18: e3000411, 2020.